Supplementary Information

Synchronized spatial shifts of Hadley and Walker circulations

Kyung-Sook Yun[1,2], Axel Timmermann[1,2], and Malte F. Stuecker[3]

[1]Center for Climate Physics, Institute for Basic Science (IBS), Busan 46241, South Korea

[2]Pusan National University, Busan 46241, South Korea

[3]Department of Oceanography and International Pacific Research Center, School of Ocean and Earth Science and Technology, University of Hawaiʻi at Mānoa, Honolulu, HI, USA

1. Strength mode for WC and HC

The first EOF of WC variability (i.e., WC1) and the second EOF mode of HC variability (i.e., HC2) represent canonical El Niño driven WC and HC variability (Supplementary Fig. S1) (e.g., Bayr et al. 2014): an anomalous clockwise cell over the eastern Indian Ocean and an anomalous anti-clockwise cell over the western Pacific, accompanied by an anomalous descending branch centered at ~ 130°E (Supplementary Fig. S1a); the equatorially symmetric HC cells with an upward motion in the equatorial region (Supplementary Fig. S1b). To focus on the El Niño-related circulation pattern, the WC1 EOF mode is reversed in sign so that positive values refer to a weakening of the WC and strengthening of the HC. Supplementary Table S1 clearly reveals the statistically significant connection between WC1-HC2 and the strength of the anomalous circulations.

2. Definition of indices for WC and HC

To measure the strength variations and spatial shifts of both the Walker circulation (WC) and Hadley circulation (HC) ascending branches, we define several indices as follows: (1) the Inter-Tropical Convergence Zone (ITCZ) position was calculated by zonal averaged latitudinal position of the ITCZ that is identified as the maximum in time-mean precipitation; (2) the ITCZ intensity is defined as zonal averaged rainfall of the ITCZ (latitudinal position defined by (1)); (3) Rainfall intensity over the Maritime continent (MC, Rain_MC) are the area-averaged precipitation anomalies over [10°S-10°N, 100°E-130°E]; (4) Rainfall intensity over the western North Pacific (WNP, Rain_WNP) are the area-averaged precipitation anomalies over [0°-15°N, 140°E-170°E]; (5) ITCZ position over the MC is the latitudinal position of the ITCZ zonally averaged over the MC [100°-130°E]; (6) WCS (Walker circulation strength) and (7) HCS (Hadley circulation strength) are respectively measured by (6) the maximum value of tropical mean [5°S-5°N] mass stream function (MSF) at 500hPa (500MSF) and by (7) the maximum of zonal mean 500MSF within the latitudinal zone of 30°S–30°N (Oort and Yienger 1996); (8) WCDS (Walker circulation dipole strength) and (9) HCDS (Hadley circulation dipole strength) are respectively defined as (8) the difference in area-

averaged tropical mean 500MSF between the central-eastern Pacific [160°E-120°W] and the Indo-western Pacific [60°E-140°E] and as (9) the difference in area-averaged zonal mean 500MSF between Northern hemisphere [NH; 5°N-25°N] and Southern hemisphere [SH; 25°S-5°S] (Ma and Yu 2014; Xie and Zhou 2017). The inter-annual correlation coefficients between indices and WC/HC PC variability are presented in Supplementary Table S1. These indices were used only in Supplementary Information.

3. Supplementary Tables and Figures

Supplementary Table S1 | Absolute correlation coefficients between inter-annual variabilities of Walker/Hadley circulations and climate indices in terms of both strength and spatial shifts. The detail for climate indices was explained in Supplementary text. The statistically significant corrections at the 95% confidence level are denoted in bold type.

Correlation coefficient	Strength mode		Shift Mode	
	Walker mode (WC1)	*Hadley mode (HC2)*	*Walker mode (WC2)*	*Hadley (HC1) mode*
ITCZ position	0.25	0.34	0.28	**0.54**
ITCZ intensity	**0.52**	**0.57**	0.23	0.15
Rainfall intensity over MC	**0.77**	**0.53**	0.01	0.12
Rainfall intensify over WNP	0.02	0.09	**0.91**	**0.63**
ITCZ position over MC	0.06	0.18	**0.52**	**0.55**
WC strength	**0.84**	**0.67**	0.08	0.05
WCDS	**0.89**	**0.78**	0.44	0.36
HC strength	**0.63**	**0.82**	0.13	0.02
HCDS	**0.60**	**0.89**	0.01	0.05

Supplementary Table S2 | Description of 19 AMIP models as part of CMIP5 used in this study. The CC indicates the inter-annual correlation coefficient between PC time series of WC2 and HC1 during 1979-2008. The strong PSYN models are denoted in bold [**], while the weak PSYN models are presented in bold [++].

#	Model	Institution	CC (WC2, HC1)
1	ACCESS1.0	CSIRO-BOM, Australia	**0.70**[**]
2	BNU-ESM	College of Global Change and Earth System Science, China	0.57
3	CMCC-CM	Centro Euro-Mediterraneo per I Cambiamenti Climatici, Italy	0.55
4	CNRM-CM5	Centre National de Recherches Météorologiques (CNRM) and Centre Europeen de Recherches et de For- mation Avancee en Calcul Scientifique (CERFACS), France	**0.67**[**]
5	CSIRO-Mk3.6.0	CSIRO-QCCCE, Australia	0.56
6	CanAM4	Canadian Centre for Climate Modelling and Analysis, Canada	0.54
7	GFDL-CM3	NOAA Geophysical Fluid Dynamics Laboratory, USA	0.48
8	GFDL-HIRAM-C180	NOAA Geophysical Fluid Dynamics Laboratory, USA	0.47
9	GISS-E2-R	NASA Goddard Institute for Space Studies, USA	0.51
10	HadGEM2-A	Met Office Hadley Centre, UK	**0.72**[**]
11	IPSL-CM5A-LR	Institut Pierre-Simon Laplace, France	0.56
12	MIROC5	MIROC, Japan	0.52
13	MPI-ESM-LR	Max-Planck-Institut für Meteorologie, Germany	0.66
14	MPI-ESM-MR	Max-Planck-Institut für Meteorologie, Germany	0.63
15	MRI-CGCM3	Meteorological Research Institute, Japan	**0.69**[**]

#	Model	Institution	CC (WC2, HC1)
16	MRI-AGCM3-2H	Meteorological Research Institute, Japan	0.37[++]
17	NorESM1-M	Norwegian Climate Centre, Norway	0.42[++]
18	BCC-CSM1.1(m)	Beijing Climate Center, China	0.32[++]
19	INM-CM4	Institute for Numerical Mathematics, Russia	0.4[++]

Supplementary Table S3 | Description of 21 AMIP models as part of the CMIP6 used in this study. The CC indicates the inter-annual correlation coefficient between PC time series of WC2 and HC1 during 1979-2014. The strong SYN models are denoted in bold [**], while the weak SYN models are presented in bold [++].

#	Model	Institution	CC (WC2, HC1)
1	BCC-CSM2-MR	Beijing Climate Center, China	0.47
2	BCC-ESM1	Beijing Climate Center, China	0.33[++]
3	CAMS-CSM1-0	Chinese Academy of Meteorological Sciences, China	0.47
4	CESM2-WACCM	National Center for Atmospheric Research, Climate and Global Dynamics Laboratory, USA	0.54
5	CESM2	National Center for Atmospheric Research, Climate and Global Dynamics Laboratory, USA	0.45
6	CanESM5	Canadian Centre for Climate Modelling and Analysis, Canada	0.56
7	ES3M-1-0	E3SM-Project, USA	0.66[**]
8	EC-Earth3-Veg	EC-Earth-Consortium,	0.41
9	FGOALS-f3-L	Chinese Academy of Sciences, China	0.57
10	GFDL-AM4	NOAA Geophysical Fluid Dynamics Laboratory, USA	0.50
11	GFDL-CM4	NOAA Geophysical Fluid Dynamics Laboratory, USA	0.59[**]

1 2	**GISS-E2-1-G**	NASA Goddard Institute for Space Studies, USA	0.34
1 3	**IPSL-CM6A-LR**	Institut Pierre-Simon Laplace, France	**0.3**[++]
1 4	**MIROC6**	MIROC, Japan	0.48
1 5	**MRI-ESM2-0**	Meteorological Research Institute, Japan	0.39
1 6	**NESM3**	Nanjing University of Information Science and Technology, China	0.35
1 7	**SAM0-UNICON**	Seoul National University, Republic of Korea	0.54
1 8	**CNRM-CM6-1**	Centre National de Recherches Météorologiques (CNRM) and Centre Europeen de Recherches et de For- mation Avancee en Calcul Scientifique (CERFACS), France	**0.19**[++]
1 9	**CNRM-ESM2-1**	CNRM-CERFACS, France	**0.08**[++]
2 0	**HadGEM3-GC31-LL**	Met Office Hadley Centre, UK	**0.64****
2 1	**UKESM1-0-LL**	Met Office Hadley Centre, UK	**0.58****

7
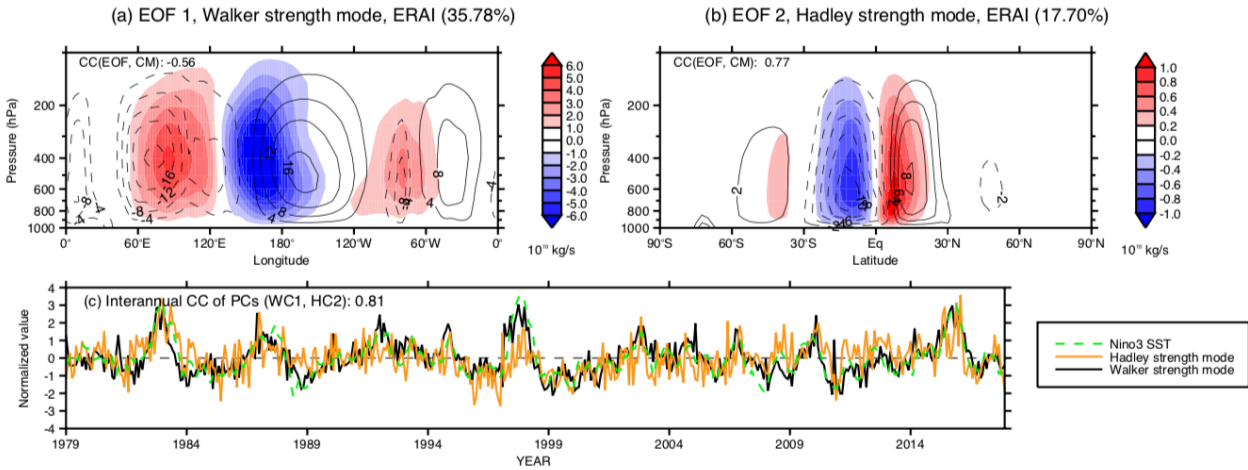
Supplementary Figure S1 | Dominant pattern of the strength modes of the Walker and Hadley circulations. (a-b) The loading patterns of the strength modes (i.e., mode 1 for Walker and mode 2 for Hadley; denoted by shading) for (a) Walker circulation (WC) and (b) Hadley circulation (HC) variability. The WC and HC are identified as (a) tropical (5°S-5°N) averaged mass stream function (MSF) anomalies and (b) zonally averaged MSF anomalies, obtained from the monthly ERA interim (ERAI) data during the period 1979-2017. The contours show the climatological mean of the MSF for the circulations. (c) Normalized time series: The corresponding principal components (PCs) of the strength modes (i.e., Walker 1 mode and Hadley 2 mode; WC1 & HC2) and Niño3 SST anomaly (green dashed line). The inter-annual correlation coefficient (CC) is ~ 0.91 for WC1-Niño3; ~ 0.87 for HC2-Niño3; ~ 0.81 between WC1 and HC2.
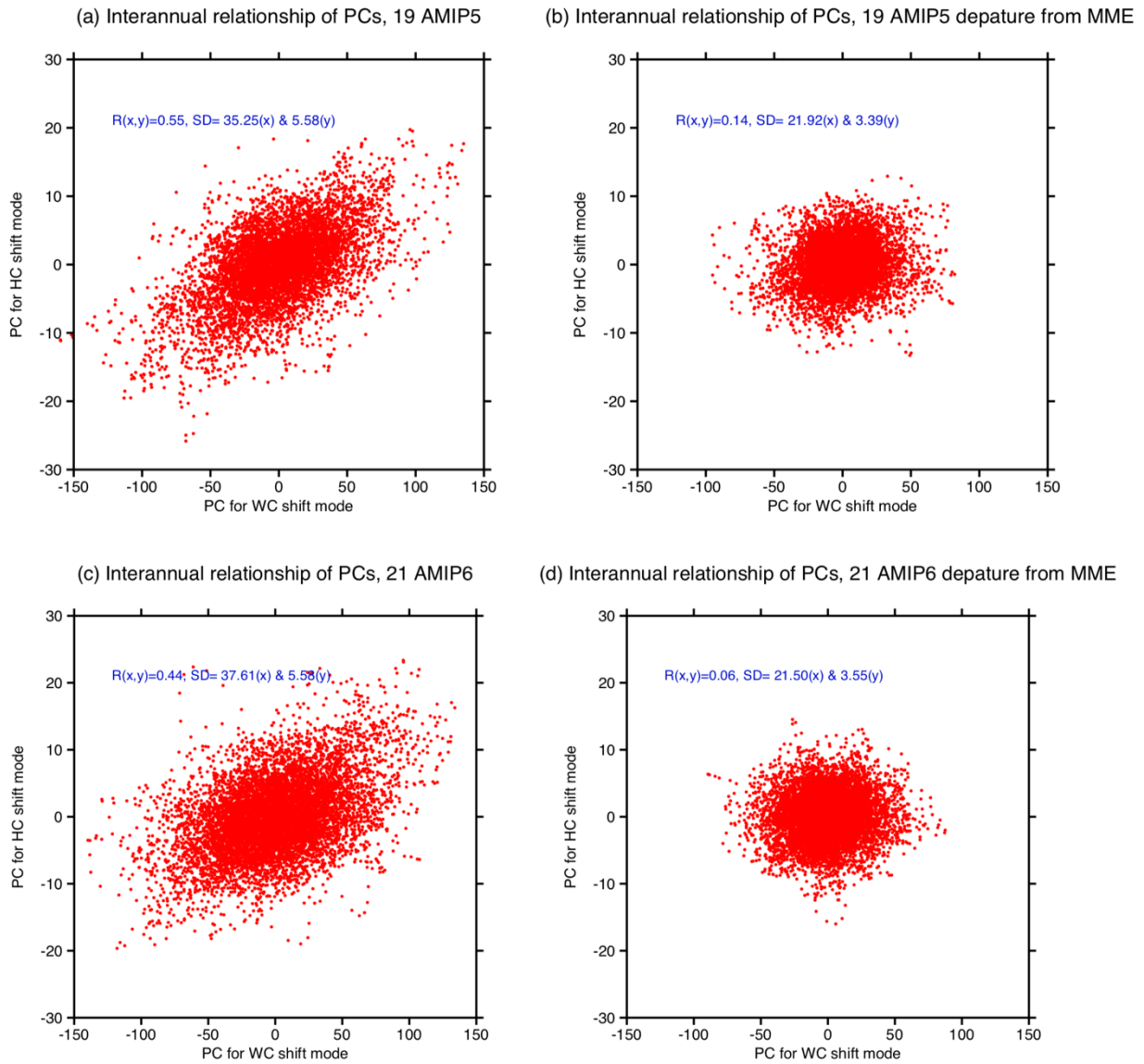
Supplementary Figure S2 | Interannual relationship between shift modes in the AMIP simulations. (a-b) Scatter plot of WC shift mode (WC2) versus HC shift mode (HC1), based on the PC time series using (a) the individual 19 AMIP5 simulations and (b) the departure from the multi-model mean (MME). (c-d) Same as (a-b), but for 21 AMIP6 simulations.

9
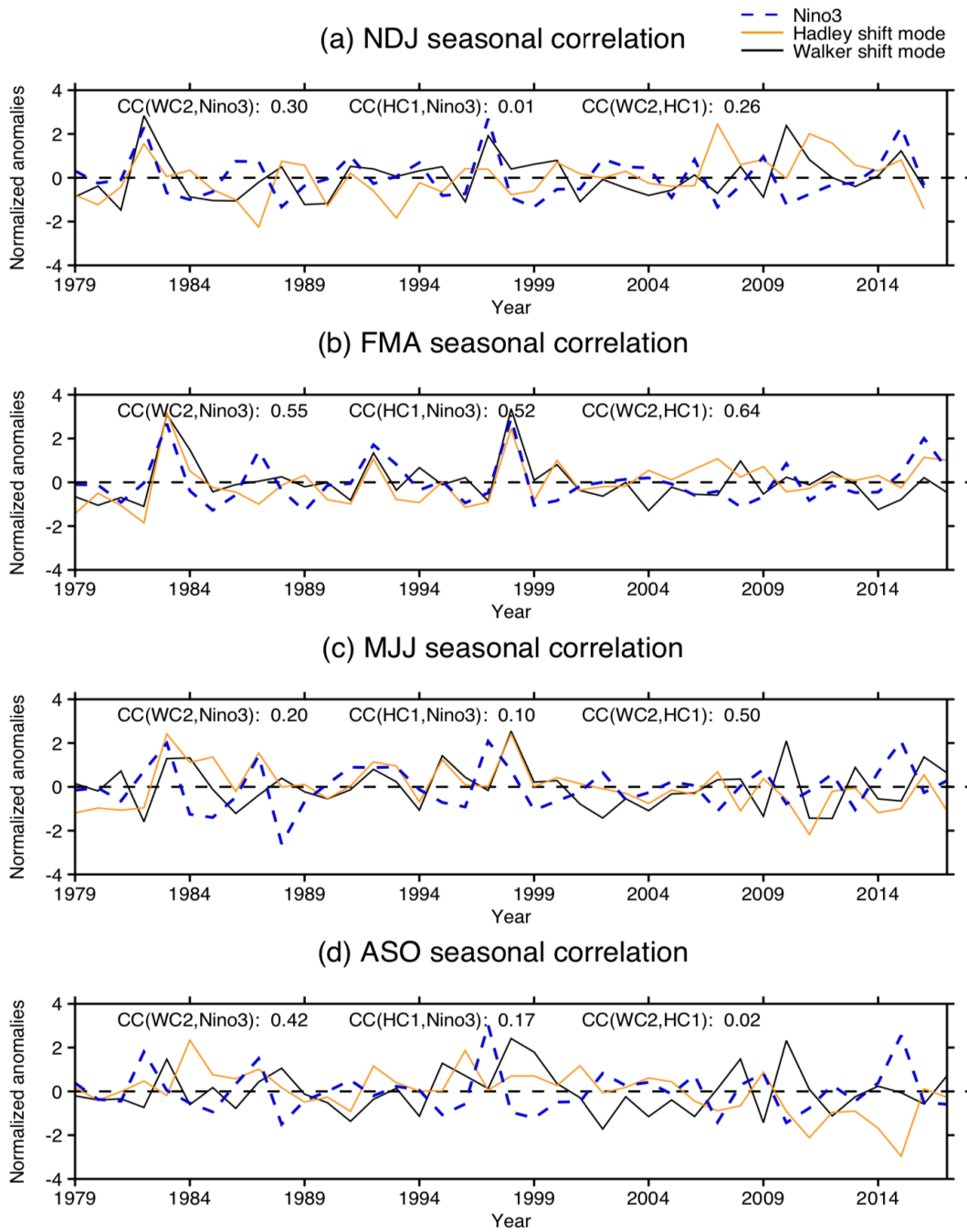
Supplementary Figure S3 | Seasonal relationship between the WC-HC shift modes and Niño3.
Seasonal mean normalized time series of Niño3 SST anomaly (blue) and the PCs of WC2 (black)
HC1 (yellow) mode: (a) November-December-January (NDJ), (b) February-March-April (FMA), (c)
May-June-July (MJJ), and (d) August-September-October (ASO).
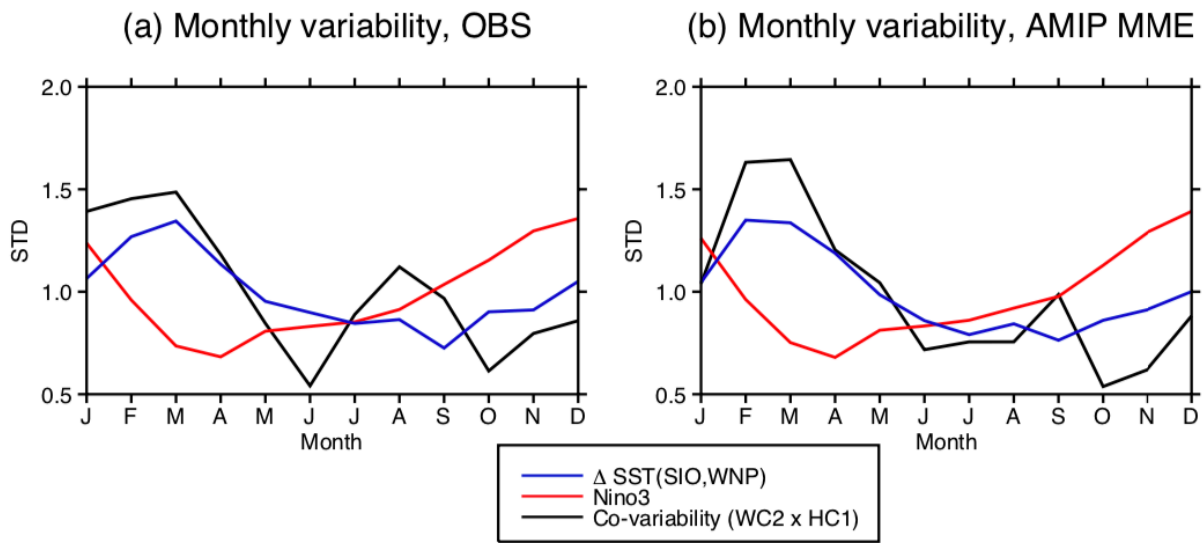
Supplementary Figure S4 | Annual cycle of WC-HC co-variability in the observations and AMIP MME. Monthly variability standard deviation of Niño3 (red), SSTgrad (blue), and WC-HC co-variability (black; product of WC2 and HC1 PCs), obtained from observations and the AMIP MME.
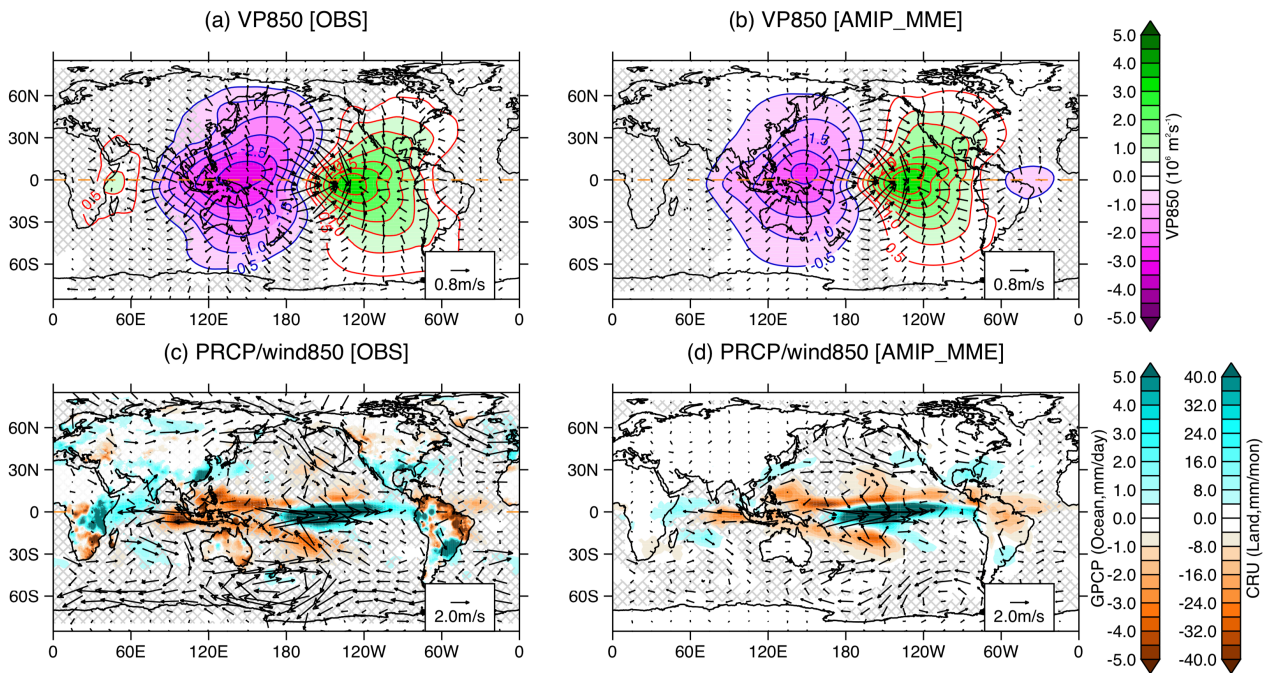
Supplementary Figure S5 | Global pattern of phase synchronized shifts during El Niño conditions. Composite anomaly of PSYN months (i.e., the absolute tendency of phase difference is less than 0.3) with November-December[0]-January[1] El Ninos (Niño3 > 1.5SD), obtained from the observations (left column) and the AMIP MME (right column): (a, b) SST (shading) and 850hPa stream function anomaly; (c, d) 850 hPa velocity potential (VP850) anomaly; (e-f) precipitation (GPCP for ocean and CRU for land; shading) and 850hPa wind (vector) anomaly. The hatching indicates differences that are statistically insignificant at the 95% confidence level.
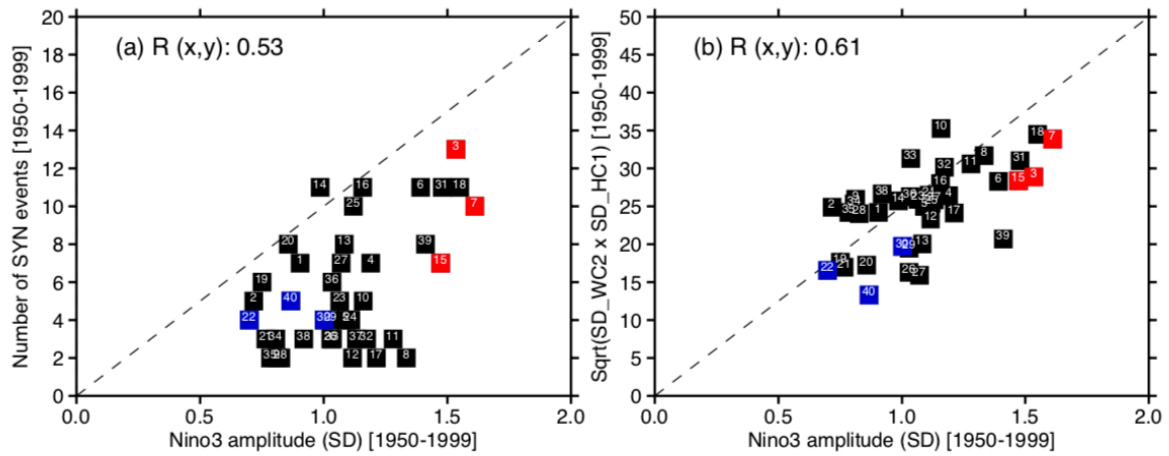
1:ACCESS1-0	2:ACCESS1-3	3:BNU-ESM	4:CCSM4	5:CESM1-BGC	6:CESM1-CAM5	7:CESM1-CAM5-1-FV2	8:CMCC-CESM
9:CMCC-CM	10:CMCC-CMS	11:CNRM-CM5	12:CSIRO-Mk3-6-0	13:CanESM2	14:FGOALS-g2	15:FIO-ESM	16:GFDL-CM3
17:GFDL-ESM2G	18:GFDL-ESM2M	19:GISS-E2-H	20:GISS-E2-H-CC	21:GISS-E2-R	22:GISS-E2-R-CC	23:HadGEM2-AO	24:HadGEM2-CC
25:HadGEM2-ES	26:IPSL-CM5A-LR	27:IPSL-CM5A-MR	28:IPSL-CM5B-LR	29:MIROC-ESM	30:MIROC-ESM-CHEM	31:MIROC5	32:MPI-ESM-LR
33:MPI-ESM-MR	34:MRI-CGCM3	35:MRI-ESM1	36:NorESM1-M	37:NorESM1-ME	38:bcc-csm1-1	39:bcc-csm1-1-m	40:inmcm4

Supplementary Figure S6 | Inter-model relationship between ENSO amplitude and WC-HC synchronization in CMIP5 models. Scatter plot of (a) the present-day (1950-1999) Niño3 SST standard deviation (SD) versus the present-day number of PSYN events and of (b) the present-day (1950-1999) Niño3 SST SD versus the present-day amplitude of the shift modes (i.e., the square root of the product of WC2 SD and HC1 SD), based on the historical simulation of the 40 CMIP5 models. The PSYN events are determined as a long-lasting phase synchronized event exceeding 6 months duration. The S3MMM group is indicated by red color and the W3MMM group by blue color. Here, S3MMM are the models that have a Niño3 SST anomaly standard deviation greater than 1.0 and high correlation between shift modes exceeding a value of 0.49, while W3MMM are models with Niño3 SST anomaly standard deviation less than 0.5.
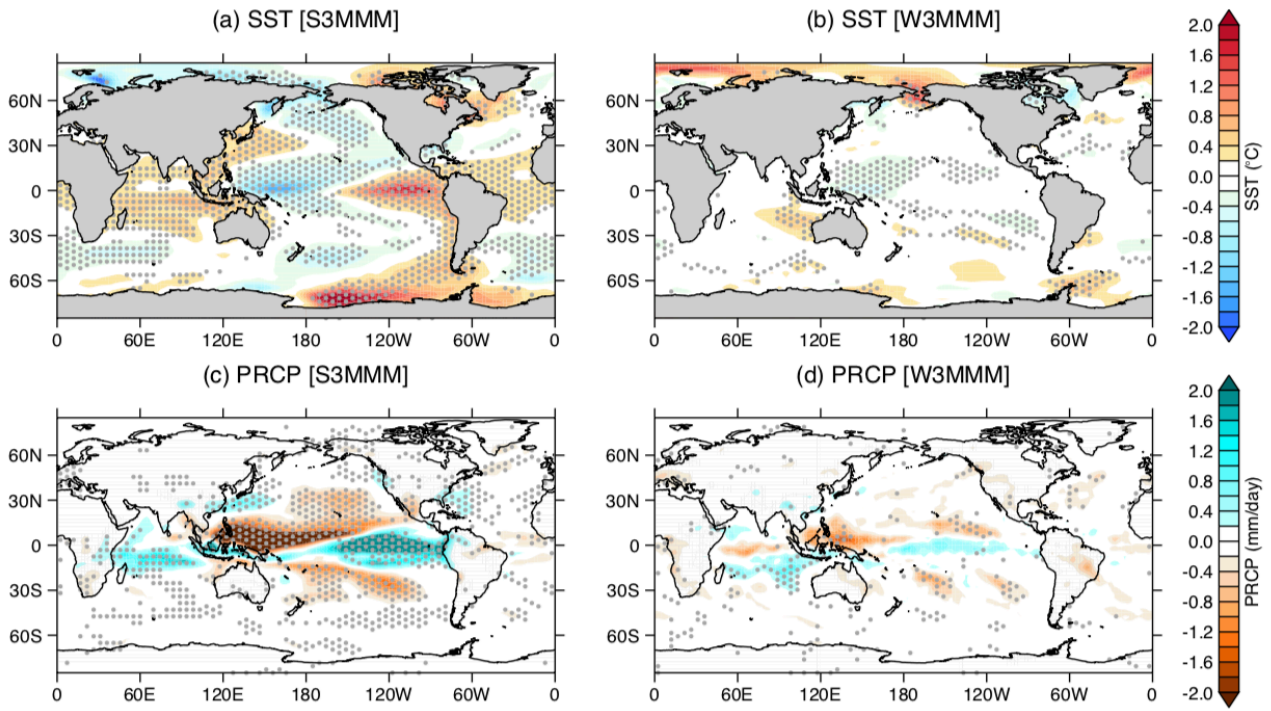
Supplementary Figure S7 | Global pattern of phase synchronized HC/WC shifts in CMIP5 models. Composite anomaly of PSYN months (i.e., the absolute tendency of phase difference is less than 0.3) with extreme SSTgrad greater than 1.5 standard deviation, for the S3MMM (left column) and W3MMM (right column) groups of the CMIP5 models: (a, b) SST (shading) and (c,d) precipitation anomalies. Stippling indicates areas where at least three models have a same signed response.
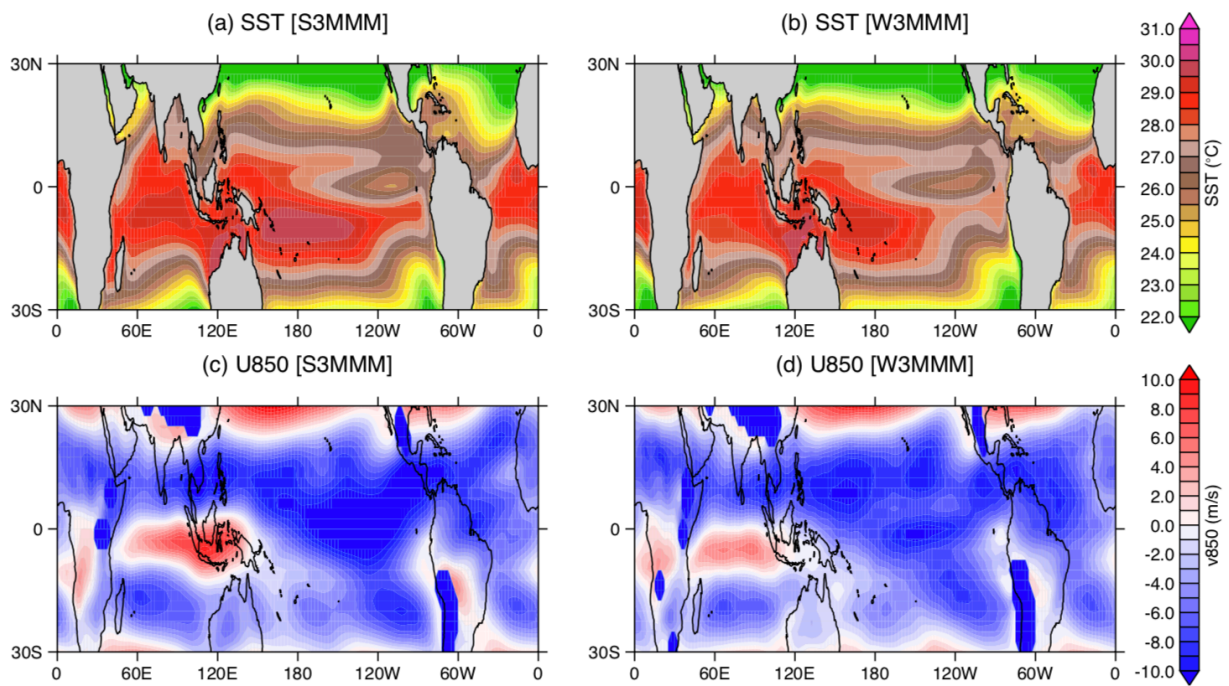
Supplementary Figure S8 | Climatological SST and zonal wind of the S3MMM and W3MMM model groups. Composite SST and 850hPa zonal wind climatology (1950-1999) for S3MMM and W3MMM.
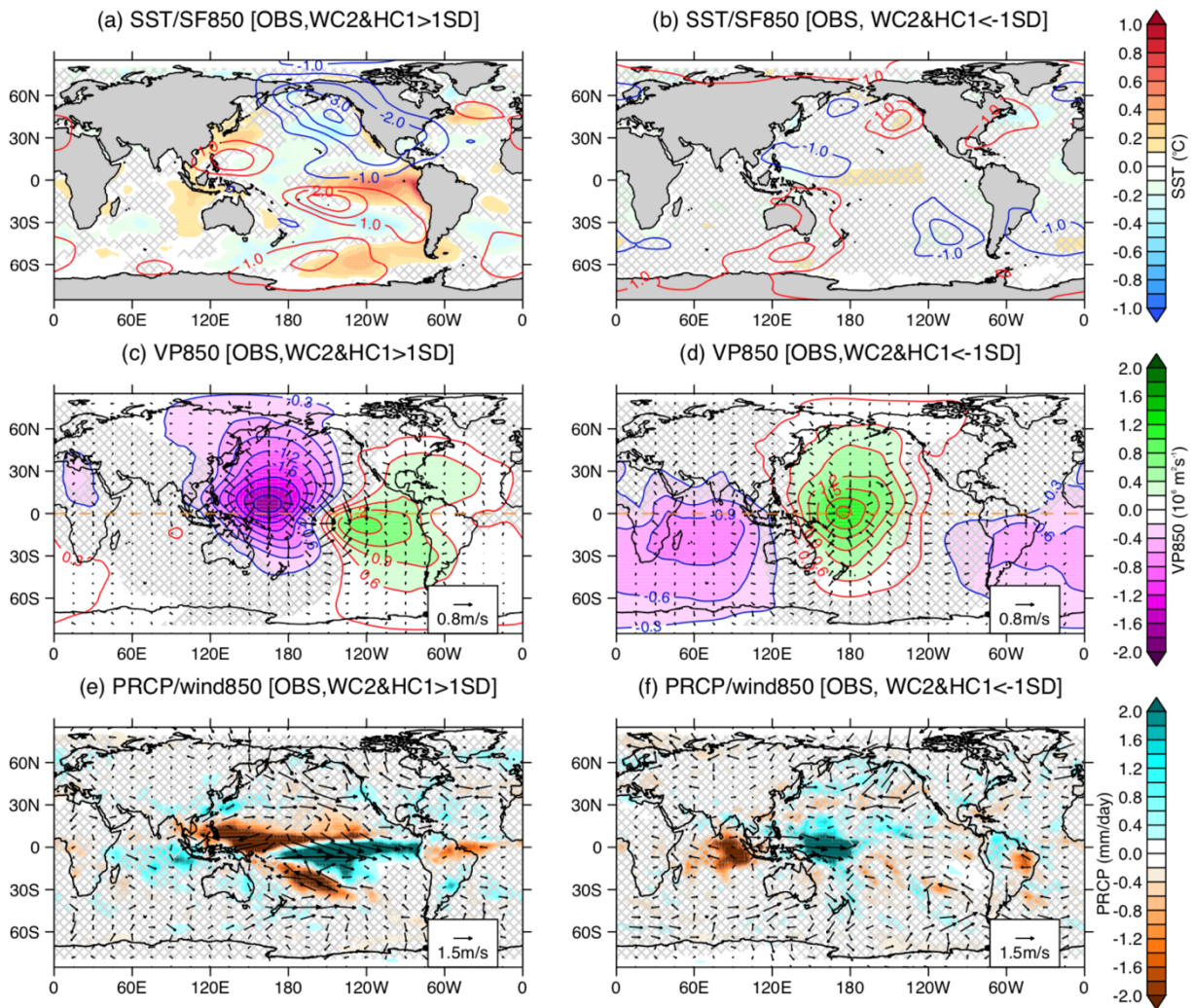
Supplementary Figure S9 | Asymmetry in the global pattern for the WC2-HC1 shift mode co-variability. (a-b) Composite anomaly during WC2-HC1 co-varying months in (left column) positive (i.e., both WC2 and HC1 greater than 1.0 standard deviation) and (right column) negative (i.e., both WC2 and HC1 less than -1.0 standard deviation) cases, obtained from the observations: (a, b) SST (shading) and 850hPa stream function anomaly; (c, d) VP850 anomaly; (e-f) GPCP precipitation (shading) and 850hPa wind (vector) anomaly. Hatching indicates areas where the difference is statistically insignificant at the 95% confidence level.
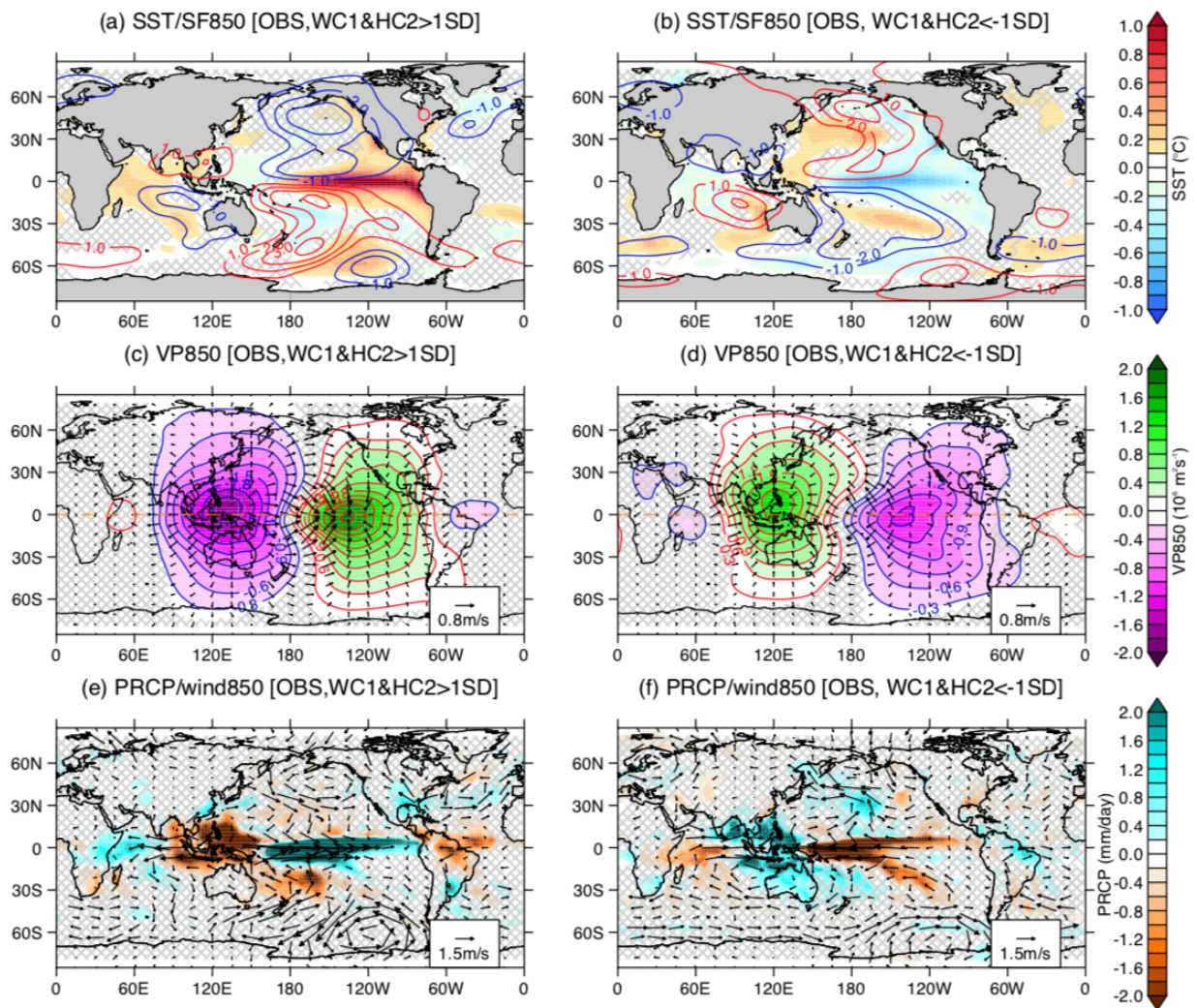
Supplementary Figure S10 | Symmetry in global pattern for WC1-HC2 strength mode co-variability. (a-b) Composite anomaly during WC1-HC2 co-varying months in (left) positive (i.e., both WC1 and HC2 greater than 1.0SD) and (right) negative (i.e., both WC1 and HC2 less than -1.0SD) cases, obtained from the observations: (a, b) SST (shading) and 850hPa stream function anomaly; (c, d) VP850 anomaly; (e-f) GPCP precipitation (shading) and 850hPa wind (vector) anomaly. The hatching shows the area where the difference is insignificant at the 95% confidence level.

Supplementary References

Bayr, T., D. Dommenget, T. Martin, and S. B. Power, 2014: The eastward shift of the Walker Circulation in response to global warming and its relationship to ENSO variability. *Climate Dynamics*, **43,** 2747-2763.

Ma, J., and J.-Y. Yu, 2014: Linking centennial surface warming patterns in the equatorial Pacific to the relative strengths of the Walker and Hadley circulations. *Journal of the Atmospheric Sciences*, **71,** 3454-3464.

Oort, A. H., and J. J. Yienger, 1996: Observed interannual variability in the Hadley circulation and its connection to ENSO. *Journal of Climate*, **9,** 2751-2767.

Xie, S.-P., and Z.-Q. Zhou, 2017: Seasonal modulations of El Niño–related atmospheric variability: Indo–western Pacific Ocean feedback. *Journal of Climate*, **30,** 3461-3472.